



Dual-layer copper mesh for integrated oil-Water separation and water purification

Haiguang Zhu, Dongyun Chen*, Najun Li, Qingfeng Xu, Hua Li, Jinghui He, Jianmei Lu*

College of Chemistry, Chemical Engineering and Materials Science, Collaborative Innovation Center of Suzhou Nano Science and Technology, Soochow University, Suzhou, 215123, China

ARTICLE INFO

Article history:

Received 6 May 2016

Received in revised form 16 July 2016

Accepted 18 July 2016

Available online 19 July 2016

Keywords:

Superhydrophobic

Photocatalytic

Oil-water separation

Water purification

ABSTRACT

One of the major environmental issues is water quality deterioration caused by the discharge of both insoluble and soluble organic pollutants, which affect human beings' health enormously. Therefore, it is of great importance to develop a versatile material to remove the organic pollutants from water. However, such materials capable of both efficiently separating insoluble oil and organic solvent from water and photodegrading soluble organic pollutions are rare on the market. Here, we report a facile method to fabricate a dual-layer copper mesh (DCM) by overlaying a graphene oxide (GO)/AgBr-coated mesh onto an Ag-coated mesh. The key point in this study is to integrate the superhydrophobic Ag-coated mesh and photocatalytic GO/AgBr-coated mesh, resulting in the bifunctional DCM with both excellent oil/water separation performance and efficient photodegradation of soluble organic pollutants under visible light illumination. Meanwhile, it is worth mentioning that the fabrication process is simple and cost-effective without using any sophisticated equipment, which permits a scale-up of DCM for water purification. Hence, the bifunctional and easily prepared properties make it an ideal candidate for encouraging application in oil/water separation and water pollutants photodegradation.

© 2016 Elsevier B.V. All rights reserved.

1. Introduction

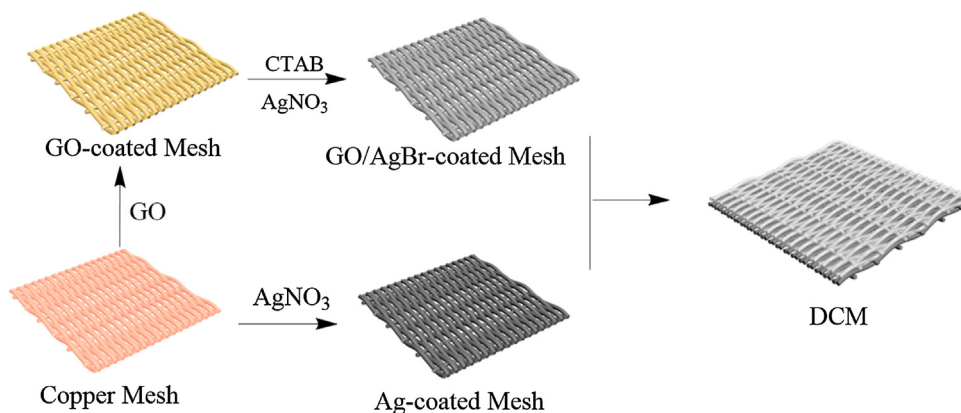
With the rapid development of industry, oil spills and chemical leakage accidents frequently occurred, which not only brought about destructive impact on ecological environment, but also presented a huge threat to the entire human community [1–8]. Thus clean-up of insoluble and soluble organic solvents from water is becoming a major problem all around the world. Therefore, effective approaches should be taken to prevent the situation from worsening. Traditional strategies, including burning, mechanical collection and the use of dispersant, have been used in removing oils and organic solvents from water. However, those methods are low efficiency and secondary pollution may occur during the clean-up process. Recently, using novel material with special wettability which exhibits opposite wettability to oil and water is becoming an ideal choice for oily wastewater treatment because of its high efficiency, low cost and chemical durability. Examples include superhydrophobic polyurethane sponge [9–11], graphene-based sponge [8,12–14], nanofibrous membrane [15–17] and so on [18–20], which exhibited high efficiency for oil adsorption

from water or oil/water separation. However, those materials with superhydrophobicity and superoleophilicity cannot treat the soluble organic pollution from wastewater. Hence, it is of great practical significance to develop a versatile material which not only can separate oils and organic solvents, but also can remove the soluble pollutants from water.

In recent years, photocatalytic techniques have been widely researched and are expected to be used for removing the soluble pollutants since the optical energy is clean and inexhaustible [21–23]. TiO₂, a traditional semiconductor photocatalyst, has been widely investigated for degradation of organic pollutants in wastewater [24–26]. However, the widely application of TiO₂ for photodegradation of pollution is still limited since the driving force is limited in UV light region. Hence, it is therefore of great importance to utilize visible light photocatalysts to provide more choices for pollution elimination and to meet several demands in practical application. Currently, silver halide, as visible-light-triggered photocatalyst, has been considered as one of the most promising material because of the excellent photocatalytic performance for the degradation of various organic pollutants. Meanwhile, in order to further enhance their photocatalytic performance, some formulated hybrids including Ag/AgBr-graphene oxide (GO) [27], Ag/AgBr-graphene [28] and Ag/AgBr-C₃N₄ [23,29,30] were fabricated.

* Corresponding author.

E-mail addresses: dychen@suda.edu.cn (D. Chen), lujm@suda.edu.cn (J. Lu).

**Scheme 1.** Schematic illustration of the fabrication process of DCM.

Herein, to address the issue that traditional oil/water materials cannot remove the soluble organic pollutants, we report a dual-layer copper mesh (DCM) that can achieve removing the oils and degradation of soluble organic pollutants from wastewater. The key strategy is to integrate photocatalytic GO/AgBr-coated mesh (upper layer) with superhydrophobic Ag-coated mesh (under layer). The fabrication process is illustrated in **Scheme 1**. Firstly, the GO was coated onto the copper mesh to prepare GO-coated mesh by simply immersing the copper mesh into GO solution and then dry at 60 °C. Then, the mesh was immersed into cetyltrimethylammonium bromide (CTAB) solution and sequentially immersed into AgNO₃ solution. After Ag⁺ reacted with Br⁻, the AgBr photocatalyst nanoparticles were successfully synthesized and homogeneously distributed on the surface of GO-coated mesh. Secondly, the superhydrophobic Ag-coated mesh was fabricated by simply immersing the copper mesh into AgNO₃ solution followed by drying treatment. The DCM was fabricated by simply overlaying the GO/AgBr-coated mesh onto the Ag-coated mesh. The AgBr nanoparticles on the surface of DCM are photocatalysts, featuring with photodegradation of organic pollutants under visible light irradiation. Meanwhile, the Ag-coated mesh owns superhydrophobic surface, which can effectively separate insoluble oils from water. As a result, under the synergistic effect between the photocatalytic GO/AgBr-coated mesh and superhydrophobic Ag-coated mesh, the DCM can not only realize the separation of oil/water mixture, but also the degradation of soluble contaminants.

2. Experimental section

2.1. Materials

Copper mesh (200 mesh) was purchased from Shanghai Yuren Co., Ltd. graphite flake (purity >99.7%), methylene blue (MB) and silver nitrate (AgNO₃) Sinopharm chemical reagent CO., Ltd (China). Sulphuric acid, phosphoric acid, potassium permanganate, H₂O₂ (30%) and cetyltrimethyl ammonium bromide (CTAB) were purchased from Chinasun Specialty Products Co., Ltd.

2.2. Instrumentation

The morphology and energy dispersive spectrometer (EDS) of copper mesh and DCM was observed using a scanning electron microscopy (SEM) (Hitachi S-4700). X-ray photoelectron spectra (XPS) were performed on an ESCALAB MK II X-ray photoelectron spectrometer using Al-K_α as the exciting source. Contact angle measurements were performed for 5 μL droplets using a JC2000D6 goniometer. TU-1901 spectrophotometer (Shimadzu) was employed for the Ultraviolet-visible (UV-vis) measurements.

2.3. Synthesis of graphene oxide (GO)

GO was synthesized according to a previous report [31]. In brief, 1.5 g graphite flake and KMnO₄ (9.0 g) were added into a 9:1 mixture of concentrated H₂SO₄/H₃PO₄ (180:20 mL). And then the mixture was magnetic stirring in an oil bath at 35 °C for 1 h and successively heated to 50 °C for 12 h. The mixture was poured into 200 mL ice water and then 30% H₂O₂ was added by dropwise until the mixture turned yellow. After that, the mixture was filtered and washed by 5% HCl for three times to remove metal ions and sequentially washed by deionized water to remove the acid. Finally, GO was obtained by freeze drying of the filter cake for 18 h.

2.4. Preparation of GO/AgBr-coated mesh

The GO-coated mesh was firstly fabricated according the previous report [32]. In brief, a circular copper mesh (diameter, 47 cm) was firstly washed with HCl (1 M) and successively washed with water. Then, the cooper mesh was immersed into GO aqueous (5 mg/mL) and the dried at 60 oC. The process was repeated for 5 times to obtain the GO-coated mesh. The obtained GO-coated mesh was immersed into 100 mL CTAB solution (8 mg/mL) at 60 oC for 5 h to synthesis the CATB functional GO-coated mesh. Finally, the CATB functional GO-coated mesh was immersed into 50 mL AgNO₃ solution (5 mg/mL) for 12 h to fabricate the GO/AgBr-coated mesh.

2.5. Preparation of Ag-coated mesh

The Ag-coated mesh was fabricated according to a simple displacement reaction by immersing the pure copper mesh into the AgNO₃ aqueous solution (1.7 mg/mL) for 30 min and then dried at 200 oC for 10 min in vacuum oven.

2.6. Photocatalytic activity test

In a typical performance, a piece GO/AgBr-coated mesh (3 × 0.5 cm) was immersed into a 4 mL methylene blue (MB) dye (10 mg/mL) aqueous solution and kept in dark for 20 min. Then, the photodegradation of test was performed using a 350W Xe lamp (XD-300) with a cut filter (>420 nm) as light source. The absorbance curves for MB solution were measured every two minutes until the peak value of absorbance curves down to the minimum level.

2.7. Water purification

The as-fabricated DCM was firstly fixed between conical flask and glass funnel. And then a 100 mL oil/water mixture (chloroform,

50% v/v) was poured into the glass funnel. After the oil was completely separated from the water, photodegradation of MB solution (10 mg/mL) was performed using the Xe lamp light source.

3. Results and discussion

The morphology of pure copper mesh, GO/AgBr-coated mesh and Ag-coated mesh was characterized by scanning electron microscopy (SEM). As shown in Fig. 1a, the pure copper mesh exhib-

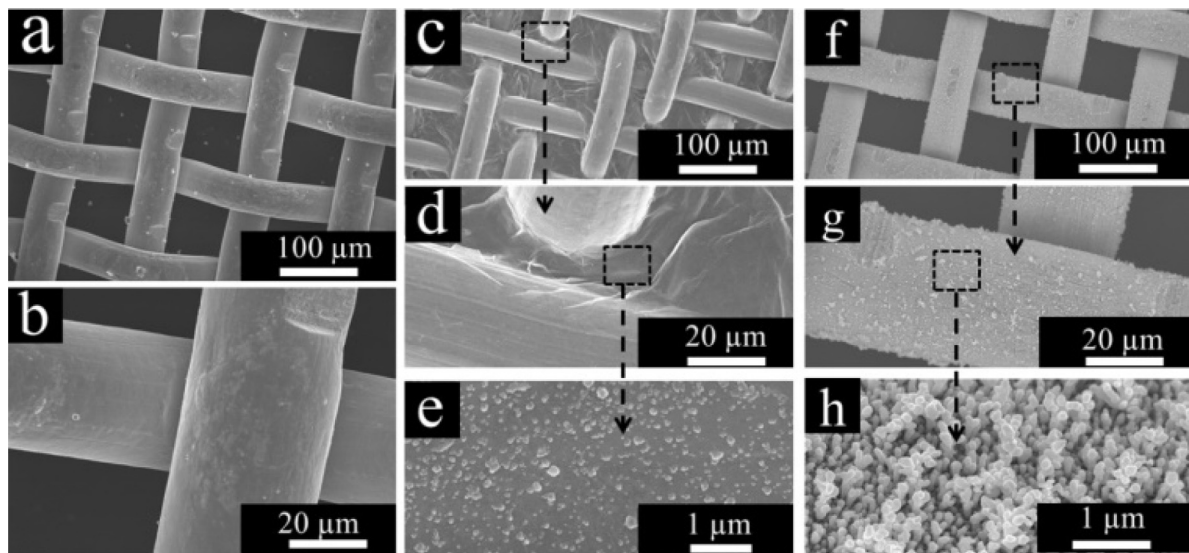


Fig. 1. SEM images of copper mesh before and after modifying nanoparticles at different magnification. (a) The image of pure copper mesh; (b) The magnified image of (a) showing the smooth surface of the pure copper mesh; (c) The image of GO/AgBr-coated mesh; (d) The magnified images of (c) revealing the presence of GO; (e) The magnified images of (d) revealing the presence of AgBr particles; (f) The image of Ag-coated copper mesh; (g and h) The magnified images of (f) revealing the presence of Ag nanoparticles.

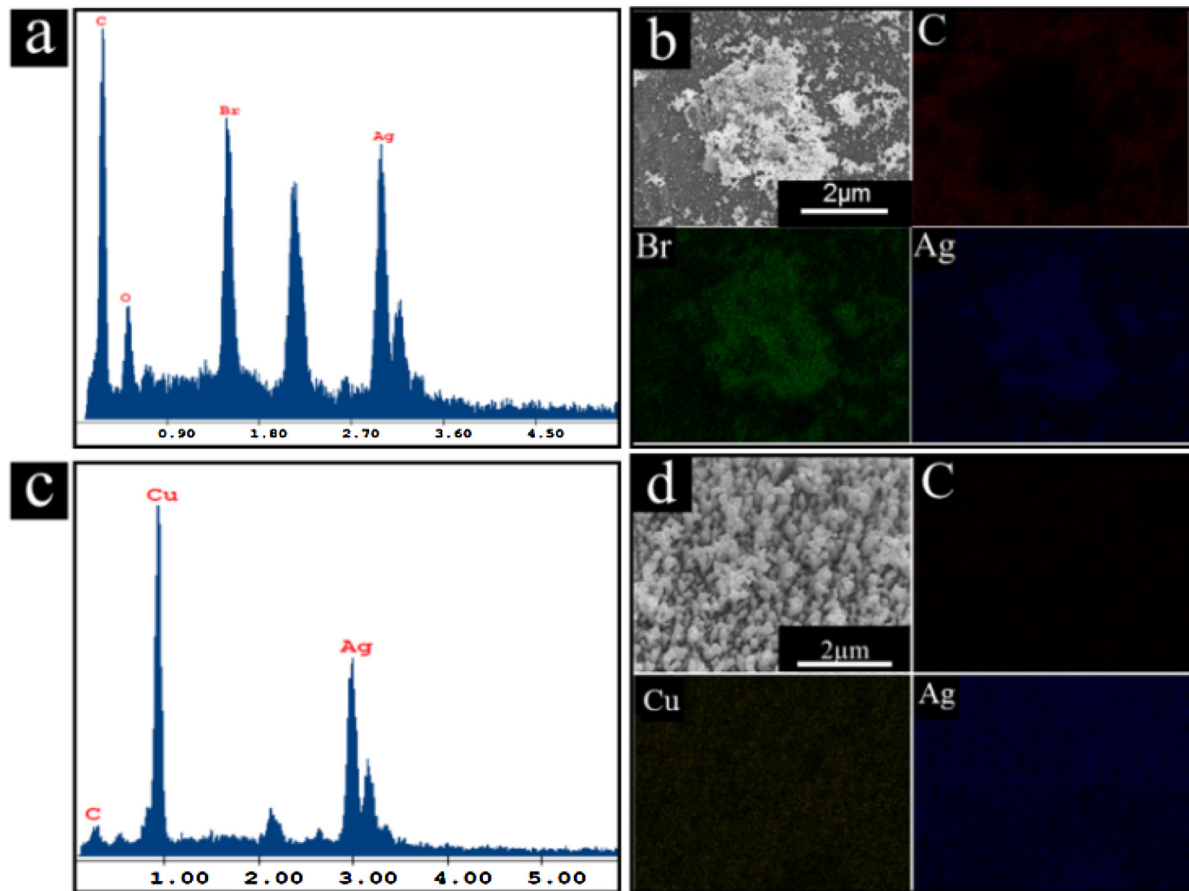


Fig. 2. The EDS image (a) and elements mapping image (b) of GO/AgBr-coated mesh; The EDS image (c) and elements mapping image (d) of Ag-coated mesh.

ited a micro-scale rough structure with an average pore diameter of 70 μm (200 mesh size). In addition, the surface of pure copper mesh is smooth and clean (Fig. 1b). After GO/AgBr coated on mesh, the pore diameter is similar as that of the initial mesh (Fig. 1c). However, it should be noted that the surface of the mesh is coated with the thin and wrinkled GO sheets, which can be further verified by the magnified view (Fig. 1d). More importantly, obvious nano/micro particles on the surface of GO are observed in the magnified view (Fig. 1e). Similarly, the pore diameters of Ag-coated mesh exhibit no obvious changes (Fig. 1f) but the rough microstructures are clearly observed in the magnified view (Fig. 1g). In addition, particles with a size of about 100–200 nm were accumulated on the surface of mesh (Fig. 1h), which resulting in the Ag-coated mesh owns multiple-scale roughness. The presence of C, O, Br and Ag elements on the surface of GO/AgBr-coated mesh and C, Ag and Cu on the Ag-coated mesh were characterized by energy dispersive spectrometer (EDS). The results were shown in Fig. 2a and c, respectively, indicating the successful synthesis of GO/AgBr nanoparticles and

Ag particles on the surface of mesh. To further identify the element distribution of GO/AgBr particles and Ag particles, element mapping were listed in Fig. 2b and d, respectively. Three mainly elements (C, Ag and Br) are obviously observed on the surface of GO/AgBr-coated mesh (Fig. 2b). Meanwhile, Cu and Ag atoms reveal a homogeneously distribution on the surface of Ag-coated mesh (Fig. 2d).

To analyze the binding energies of Ag on the surface of DCM, XPS analysis was carried out to examine the surface chemical components of pure copper mesh and DCM. As shown in Fig. 3a, copper, oxygen and carbon were detected both on surface of pure copper

and DCM. However, an obvious silver signal was detected both on the surface of GO/AgBr-coated mesh and Ag-coated mesh, confirming the successful synthesis of AgBr and Ag practices on surface of the DCM. Meanwhile, the high-resolution XPS spectrums of Ag 3d on the surface of Ag-coated mesh and GO/AgBr-coated mesh were shown in Fig. 3b and Fig. 3c, respectively. Two peaks at ca. 374.6 eV and 368.6 eV can be attributed to $\text{Ag } 3\text{d}_{3/2}$ and $3\text{d}_{5/2}$ of Ag^0 , respectively [33]. Besides, Fig. 3c display that two peaks at ca. 378.8 eV and 367.8 eV are assigned to Ag^+ of AgBr practices on surface of GO/AgBr-coated mesh. Similar to Ag 3d, the Br 3d spectrum in Fig. 3d display two peaks at ca. 69.2 eV and 68.2 eV which ascribed to $\text{Br } 3\text{d}_{3/2}$ and $3\text{d}_{5/2}$ [28].

As known to all, the roughness of surface and chemical composition play a crucial role in achieving extreme wettability [34,35]. Generally, the hydrophobicity or hydrophilicity is governed by its surface chemical composition, which can further amplify this property to superhydrophobicity or superhydrophilicity by enhancing the roughness of surface. To verify the wettability of DCM, oil and water droplets were dropped on the surface of GO/AgBr-coated mesh and Ag-coated mesh. As can be seen in Fig. 4a, both oil and water droplets were completely penetrate the GO/AgBr-coated mesh, indicating that it owns amphiphilicity. In contrast, when oil and water droplets were applied to the Ag-coated mesh, the water droplets were blocked and stayed on the surface with near-spherical shapes (Fig. 4b). And the oil can penetrate quickly, indicating it possess excellent hydrophobicity and oleophilicity. To precisely measure the wettability of DCM, Contact angle (CA) measurement was conducted by dropped a 5 μL water droplet on surface of GO/AgBr-coated mesh and Ag-coated mesh. The inset in Fig. 4a shows a tilted water droplet with a CA of 20° on the GO/AgBr-

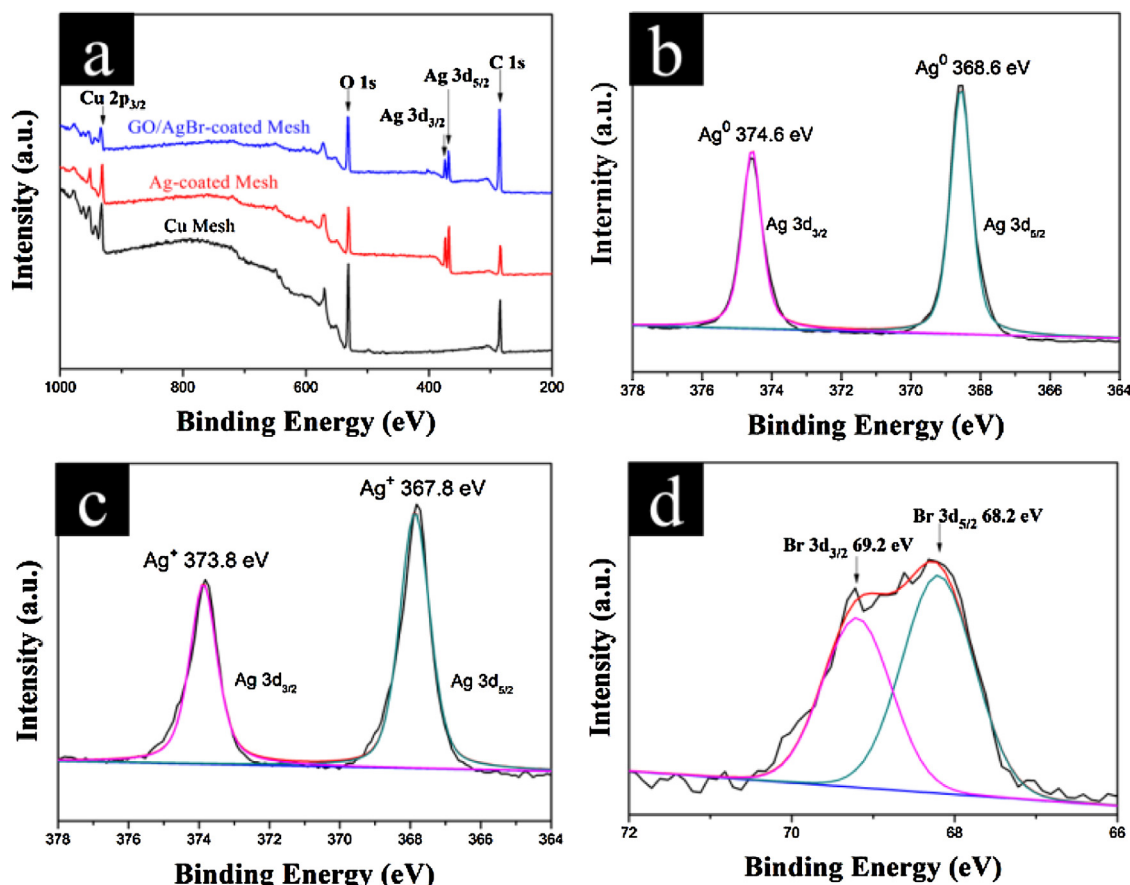


Fig. 3. (a) XPS survey spectra of copper mesh and DCM; (b) XPS spectrum of Ag 3d on the surface of Ag-coated mesh; XPS spectrum of Ag 3d (c) and Br 3d (d) on the surface of GO/AgBr-coated mesh.

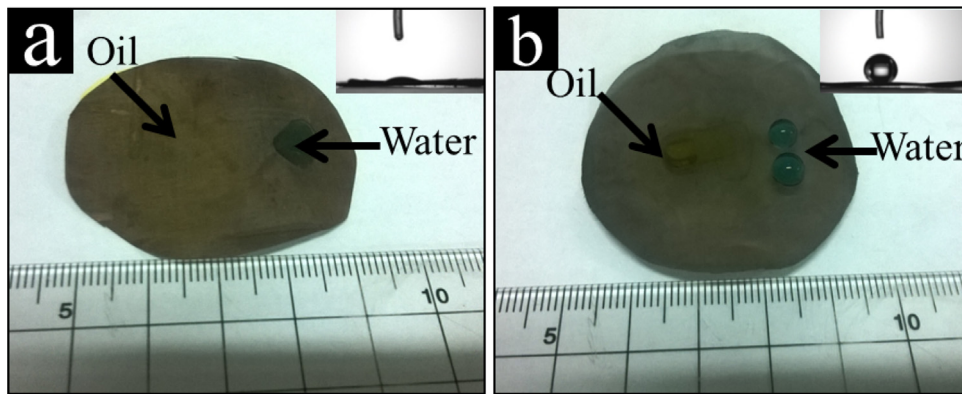


Fig. 4. (a) Image of oil droplets (left) and water droplets (right) on the surface of GO/AgBr-coated mesh. Inset: CA measurement for GO/Ag-coated mesh with a CA = 20°. (b) Image of oil droplets (left) and water droplets (right) on the surface of Ag-coated mesh. Inset: CA measurements for Ag-coated mesh with a CA = 154°.

coated mesh, which can be attributed to the hydrophilic GO on its surface. Generally speaking, to achieve the separation of oils and water, materials with the opposite wettability to oils and water is a necessity. For separation or collection of oils from oils/water mixture, membrane with superhydrophobicity and superoleophilicity is an ideal material because it can selectively filter the oils while block the water. As well known, rough structure and low surface energy are two key factors to obtain the surface with superhydrophobicity. For the as-prepared Ag-coated mesh, it exhibited multiple-scale rough structure due to a large number of silver particles accumulated on the surface of mesh. Furthermore, the silver particles can adsorb hydrocarbons from ambient air during the heating [33], which can be confirmed from the high-resolution XPS C 1 s spectrum of Ag-coated mesh (Fig. S1). Since nonpolar organic reagent with low surface energy were adsorbed and deposited on the surface of silver particles, the Ag-coated mesh is believed to possess excellent hydrophobicity, which further amplified its roughness surface. As shown in the inset of Fig. 4b, a water droplet formed a sphere with a CA 154° on the surface of Ag-coated mesh, which make oils or organic solvents pass through the Ag-coated mesh more easily; on the contrary, the polar water was blocked on the surface of the mesh, which promised the potential application in oil/water separation.

As has been reported, AgX (X=Cl, Br) nanoparticles have excellent photocatalytic property in degradation of organic contaminants under visible light illumination. Therefore, methylene

blue (MB), a heterocyclic aromatic organic compound, was used a target molecule to evaluate the photocatalytic activity of AgBr particle on surface of GO/AgBr-coated mesh. As shown in Fig. 5a, the concentration of MB aqueous solution, which can be reflected by the absorbance of visible light according to Lambert-Beer law, decreased its initial value to 30% after light illumination for 2 min and completely declined to zero 8 min later, indicating its excellent photodegradation for MB pollutions. Meanwhile, the recyclability of the GO/AgBr-coated mesh is key criteria for practical application for photodegradation of organic pollutants. Fig. 5b shows the reuse behavior of GO/AgBr-coated mesh for photodegradation of MB aqueous solution for five times, indicating that its excellent recyclability for photodegradation of organic pollutants. In addition, an obvious growth of photocatalytic activity along with the increasing cycling number in the first three circulation process has been demonstrated in Fig. 5b, which is attributed to the generation of metallic Ag⁰ during the photodegradation process (Fig. S2a). The high-resolutions of XPS spectrum of Ag 3d demonstrated that ca. 6.3% content of Ag⁰ was produced after photodegradation of MB (Fig. S2b). As reported previously, GO was suggested to be an ideal supporting material to stabilize metal nanoparticles and also could endow the composite materials with high electron mobility, large surface area, superior durability as well as efficient electron-hole separation properties, resulting in excellent photocatalytic activity [36–39]. The contribution of GO to photodegradation of MB was investigated and shown in Fig. S3, the original MB (10 mg/mL) can

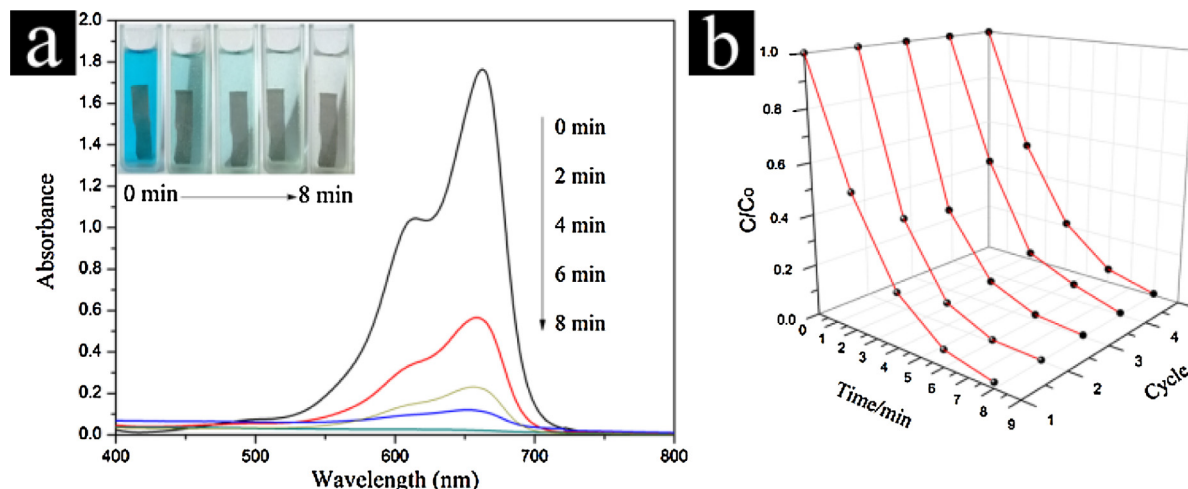
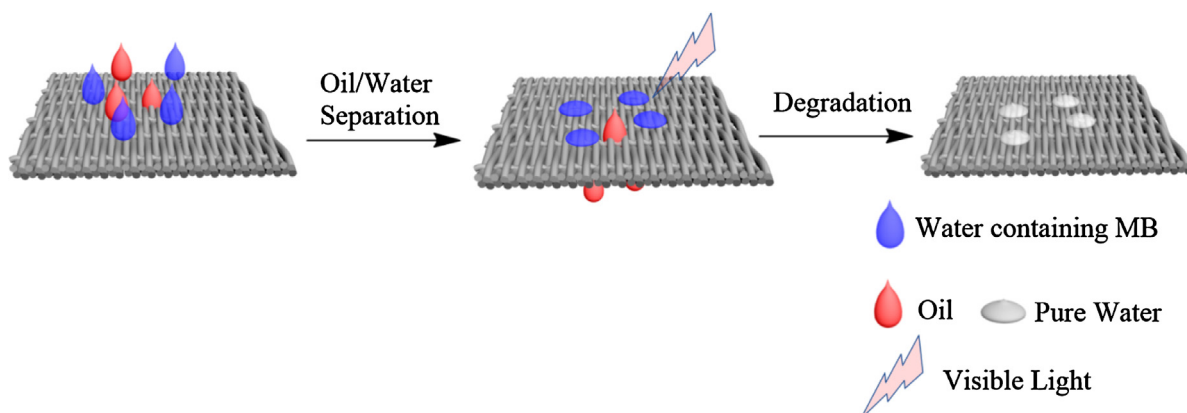


Fig. 5. (a) The temporal absorbance curves for MB solution (4 mL, 10 mg/L) during the photodegrade process. The inset: the typical real-time images during the photodegradation of MB solution by the GO/AgBr-coated mesh (3 × 0.5 cm). (b) Five successive cycling photodegradation dynamic curves of MB for the GO/AgBr-coated mesh.



Scheme 2. Schematic illustration of separation of oil/water mixture and degradation of soluble contaminations by using the DCM.

be completely degraded by the GO/AgBr composite photocatalyst under visible light illumination for *ca.* 8 min, while *ca.* 73% of MB molecules were degraded by the pristine AgBr under the similar conditions. The results indicated that the existence of GO can obviously enhance the photocatalytic activities of AgBr photocatalysts.

By integrating the photodegradation property of GO/AgBr-coated mesh and superhydrophobicity property of Ag-coated mesh, the as-designed DCM could exhibit bifunctional property both in oil/water separation and degradation of organic pollution. To illustrate this, a model for water purification was designed and showed in **Scheme 2**, as the upper layer mesh is the amphiphatic materials, oil and water can easily penetrate the mesh. When touched the oil/water mixture. However, the water is blocked by the superhy-

drophobic Ag-coated mesh (under layer) and the oil can continue to penetrate the as-prepared DCM to achieve the separation of oil/water mixture. Meanwhile, owing to the AgBr nanoparticles on the surface of the upper layer mesh are excellent photocatalysts for the degradation of pollutants, the water stayed on the surface of DCM can further purification by photocatalytic degradation of soluble pollution under visible light illumination. As a proof-of-concept, 100 mL oil/water mixture (chloroform, 50% v/v) was poured into the vessel, as shown in **Fig. 6a**, insoluble oil could easily penetrate the as-prepared DCM (Movie.1), leaving the water (containing MB, 10 mg/L) on the surface of DCM. And the insoluble organic contaminants were sequentially degraded under visible light irradiation, leaving transparent water after light irradiation for 50 min

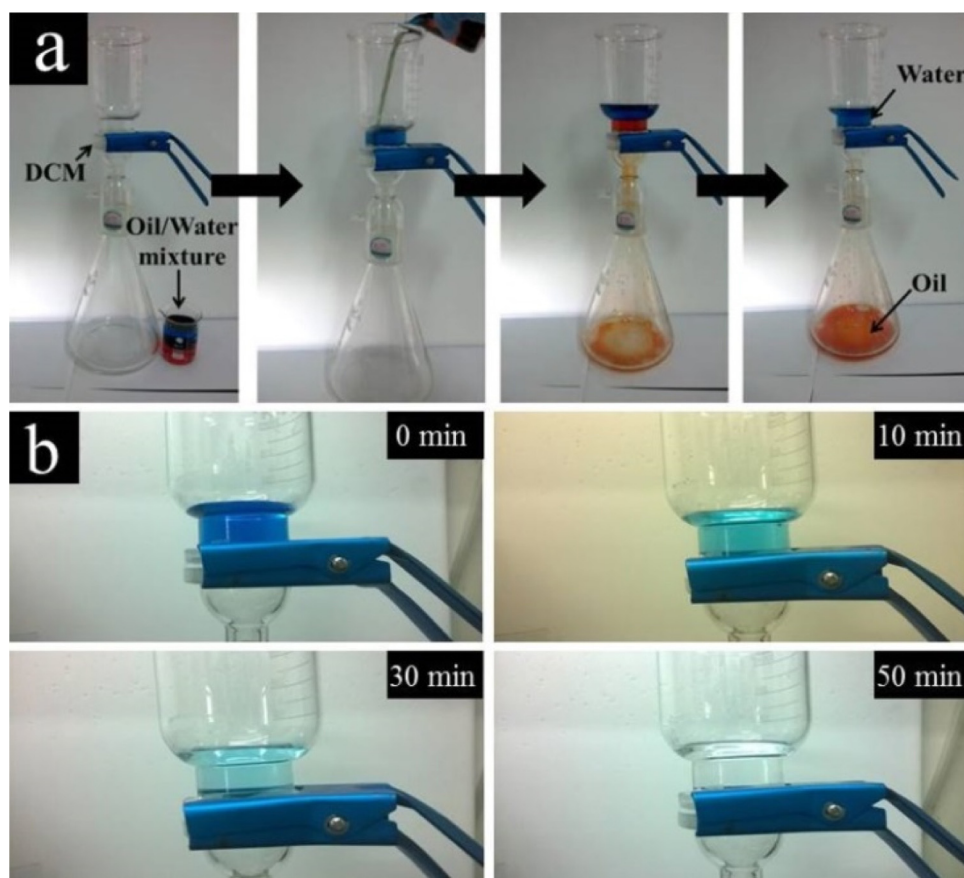


Fig. 6. Water purification by DCM. (a) Screenshots of the movie showing the oil/water separation by DCM (oil was stain with Sudan red). (b) The typical real-time figures of successive photodegradation of MB. (For interpretation of the references to colour in this figure legend, the reader is referred to the web version of this article.)

(Fig. 6b). To further verify the practicability of DCM for water purification, separation tests of DCM for various organic solvents, such as chloroform, dichloromethane and hexane, were carried out and the results were shown in Fig. S4, the as-prepared DCM exhibited excellent separation performance for common organic solvent. And the separation efficiency, defined as $(W_{\text{after}} - W_{\text{before}}) \times 100\%$, where W_{before} and W_{after} are the weight of organic solvents before and after separation test, respectively, can reach up to 99%. Moreover, the Ag-coated mesh maintained excellent hydrophobicity with a CA of approximately 140° after three times separation tests for each organic solvent. The result suggests that the as-prepared DCM exhibit promising application in water purification by separation of insoluble oil or organic solvents and photodegradation of soluble organic contaminants.

4. Conclusions

In summary, bifunctional copper mesh with both superhydrophobicity and photodegradation was successfully fabricated by integrating the photocatalytic GO/AgBr-coated mesh and superhydrophobic Ag-coated mesh. The possible synergistic effect of the meshes rendered the as-fabricated DCM not only with excellent efficiency for separation of insoluble oils, but also with outstanding photodegradation of soluble organic pollutants from wastewater. And we believe that the attractive features of as-fabricated DCM make it an ideal candidate for water purification.

Acknowledgements

We gratefully acknowledge the financial support provided by National Natural Science Foundation of China (21336005, 21301125, and 51573122), Natural Science Foundation of the Education Committee of Jiangsu Province (15KJB150026), Environmental Protection Research Foundation of Suzhou, and Suzhou Nano-project (ZXG2013001, ZXG201420).

Appendix A. Supplementary data

Supplementary data associated with this article can be found, in the online version, at <http://dx.doi.org/10.1016/j.apcatb.2016.07.028>.

References

- [1] Y. Yu, H. Chen, Y. Liu, V.S.J. Craig, C. Wang, L.H. Li, Y. Chen, *Adv. Mater. Interfaces* 2 (2015) 1400267.

- [2] L.L. Zhu, C.F. Tan, M.M. Gao, G.W. Ho, *Adv. Mater.* 27 (2015) 7713–7719.
- [3] D. Liu, L. He, W. Lei, K.D. Klika, L. Kong, Y. Chen, *Adv. Mater. Interfaces* (2015).
- [4] W. Liang, Z. Guo, *RSC Adv.* 3 (2013) 16469–16474.
- [5] A. Jerneiöv, *Nature* 466 (2010) 182–183.
- [6] Z.X. Wang, C.H. Lau, N.Q. Zhang, Y.P. Bai, L. Shao, *J. Mater. Chem. A* 3 (2015) 2650–2657.
- [7] J. Wang, L. Shang, Y. Cheng, H. Ding, Y. Zhao, Z. Gu, *Small* 11 (2015) 3890–3895.
- [8] H. Bi, X. Xie, K. Yin, Y. Zhou, S. Wan, L. He, F. Xu, F. Banhart, L. Sun, R.S. Ruoff, *Adv. Funct. Mater.* 22 (2012) 4421–4425.
- [9] B. Li, L. Li, L. Wu, J. Zhang, A. Wang, *ChemPlusChem* 79 (2014) 850–856.
- [10] Q. Zhu, Y. Chu, Z. Wang, N. Chen, L. Lin, F. Liu, Q. Pan, *J. Mater. Chem. A* 1 (2013) 5386–5393.
- [11] C.F. Wang, S.J. Lin, *ACS Appl. Mater. Interfaces* 5 (2013) 8861–8864.
- [12] H. Hu, Z. Zhao, Y. Gogotsi, J. Qiu, *Environ. Sci. Technol. Lett.* 1 (2014) 214–220.
- [13] X. Dong, J. Chen, Y. Ma, J. Wang, M.B. Chan-Park, X. Liu, L. Wang, W. Huang, P. Chen, *Chem. Commun.* 48 (2012) 10660–10662.
- [14] P. Zhai, H. Jia, Z. Zheng, C.C. Lee, H. Su, T.C. Wei, S.P. Feng, *Adv. Mater. Interfaces* 2 (2015) 1500243.
- [15] H. Wang, H. Zhou, H. Niu, J. Zhang, Y. Du, T. Lin, *Adv. Mater. Interfaces* (2015).
- [16] M.H. Tai, P. Gao, B.Y. Tan, D.D. Sun, J.O. Leckie, *ACS Appl. Mater. Interfaces* 6 (2014) 9393–9401.
- [17] X. Tang, Y. Si, J. Ge, B. Ding, L. Liu, G. Zheng, W. Luo, J. Yu, *Nanoscale* 5 (2013) 11657–11664.
- [18] J. Zhang, S. Seeger, *Adv. Funct. Mater.* 21 (2011) 4699–4704.
- [19] X. Zhou, Z. Zhang, X. Xu, F. Guo, X. Zhu, X. Men, B. Ge, *ACS Appl. Mater. Interfaces* 5 (2013) 7208–7214.
- [20] G. Ju, M. Cheng, F. Shi, *NPG Asia Mater.* 6 (2014) e111.
- [21] W. Zou, L. Zhang, L. Liu, X. Wang, J. Sun, S. Wu, Y. Deng, C. Tang, F. Gao, L. Dong, *Appl. Catal. B: Environ.* 181 (2016) 495–503.
- [22] V.K. Gupta, T.A. Saleh, D. Pathania, B.S. Rathore, G. Sharma, *Ionics* 21 (2014) 1787–1793.
- [23] H. Xu, J. Yan, Y. Xu, Y. Song, H. Li, J. Xia, C. Huang, H. Wan, *Appl. Catal. B: Environ.* 129 (2013) 182–193.
- [24] Z. Ma, W. Chen, Z. Hu, X. Pan, M. Peng, G. Dong, S. Zhou, Q. Zhang, Z. Yang, J. Qiu, *ACS Appl. Mater. Interfaces* 5 (2013) 7527–7536.
- [25] J. Liu, H. Bai, Y. Wang, Z. Liu, X. Zhang, D.D. Sun, *Adv. Funct. Mater.* 20 (2010) 4175–4181.
- [26] X. Li, G. Chen, L. Yang, Z. Jin, J. Liu, *Adv. Funct. Mater.* 20 (2010) 2815–2824.
- [27] M. Zhu, P. Chen, M. Liu, *ACS Nano* 5 (2011) 4529–4536.
- [28] Y. Fan, W. Ma, D. Han, S. Gan, X. Dong, L. Niu, *Adv. Mater.* 27 (2015) 3767–3773.
- [29] Y. Xu, H. Xu, J. Yan, H. Li, L. Huang, J. Xia, S. Yin, H. Shu, *Coll. Surf. A: Physicochem. Eng. Asp.* 436 (2013) 474–483.
- [30] J. Cao, Y. Zhao, H. Lin, B. Xu, S. Chen, *Mater. Res. Bull.* 48 (2013) 3873–3880.
- [31] C.D. Marcano, D.V. Kosynkin, J.M. Berlin, A. Stintzskii, Z.Z. Sun, B. Alemany, J.M. Tour, *ACS Nano* 4 (2010) 4806–4814.
- [32] Y. Dong, J. Li, L. Shi, X. Wang, Z. Guo, W. Liu, *Chem. Commun.* 50 (2014) 5586–5589.
- [33] F. Wang, S. Lei, Y. Xu, J. Ou, *Chempyschem* 16 (2015) 2237–2243.
- [34] L. Zhang, Z. Zhang, P. Wang, *NPG Asia Mater.* 4 (2012) e8.
- [35] B. Wang, W.X. Liang, Z.G. Guo, W.M. Liu, *Chem. Soc. Rev.* 44 (2015) 336–361.
- [36] F. Perreault, A. Fonseca de Faria, M. Elimelech, *Chem. Soc. Rev.* 44 (2015) 5861–5896.
- [37] Y. Shen, Q. Fang, B. Chen, *Environ. Sci. Technol.* 49 (2014) 67–84.
- [38] N. Zhang, Y. Zhang, Y.J. Xu, *Nanoscale* 4 (2012) 5792–5813.
- [39] N. Zhang, M.Q. Yang, S. Liu, Y. Sun, Y.J. Xu, *Chem. Rev.* 115 (2015) 10307–10377.